Electronic Supplementary Information for *Soft Matter* manuscript: Coarse-grained molecular dynamics simulations of immobilized micelle systems

Devashish Gokhale[a], Ian Chen[b] and Patrick S. Doyle[a,*]

[a]*Department of Chemical Engineering, Massachusetts Institute of Technology, Cambridge, MA 02139 (USA)*
[b]*Department of Materials Science and Engineering, Massachusetts Institute of Technology, Cambridge, MA 02139 (USA)*
*Email: pdoyle@mit.edu

Table of Contents:

SI.01: Aggregation number validation:

Surfactant	Obtained value	Literature value
L64	1.75	2[1]
C_8E_4	46	40 to 50[2]
Span 20	33	35[3]
Span 80	33	53[3]

SI.02: Effect of box size on aggregation number

Box size (measured in # Span 20 molecules (2.5% v/v in water))	Aggregation number
100	33
150	33
200	30

SI.03: Topology of representative surfactants:

B25, P85, Span 20, Tween 20, attached as separate .itp files.

SI.04: Topology of small hydrophobic molecules:

DCP, NOL, PFOA, BPA, EDOL, attached as separate .itp files.

SI.05: CMCs of surfactants:

Surfactant	CMC (mol/L)
Alkyl-PEO surfactants	
L10	1.44E-02
C10	1.46E-04
L23	6.31E-03
C20	7.12E-04
S20	6.08E-04
B25	N/A
L31	2.00E-02
PEO-PPO-PEO surfactants	
L44	3.60E-03
L61	1.10E-04
L64	8.80E-03

L92	6.50E-05
P85	8.80E-05
F68	4.80E-04
F127	2.80E-06
Sorbitan-ester surfactants	
SPAN20	3.47E-04
SPAN80	2.80E-04
TWEEN20	4.88E-05
TWEEN80	9.90E-06

SI.06: Replacing restricted bending potentials with polynomials:

The relevant molecule topologies impose a G96 potential and a restricted bending potential the EO bead of the surfactants of interest. We wish to replace both potentials with a single quartic potential to enable the calculation of free energies.

First, simulations are run starting with self-assembled systems in the absence of micropollutants, at equilibrium, using two exemplar surfactants B25 and F68 and the average bond angle energy and standard deviation of the bond angle energy stored in the G96 and restricted bending angles are recorded. It is assumed, based on the .itp topology, that the distribution of angles sampled in the simulation is a normal distribution. The mean and standard deviation of the normal distribution of angles is then fit so that the measured averages and standard deviations of bond angle energies can be reproduced. The mean in both cases is 135º, and the standard deviations are 7.7º for the restricted bending angles and 12.4º for the G96 angles. The mean standard deviation is 10º. The same values are obtained for both B25 and F68 systems.

Now, we fit a quartic potential (a fourth-order polynomial) to the restricted bending + G96 potential, minimizing the sum of squares of errors in values of the potential (y-axis in figure S4), with angles (x-axis in figure S1) sampled from a normal distribution with mean 135º and standard deviation 10º. This ensures that greater weight is given in the regression to angles which are sampled more frequently in the course of the simulation.

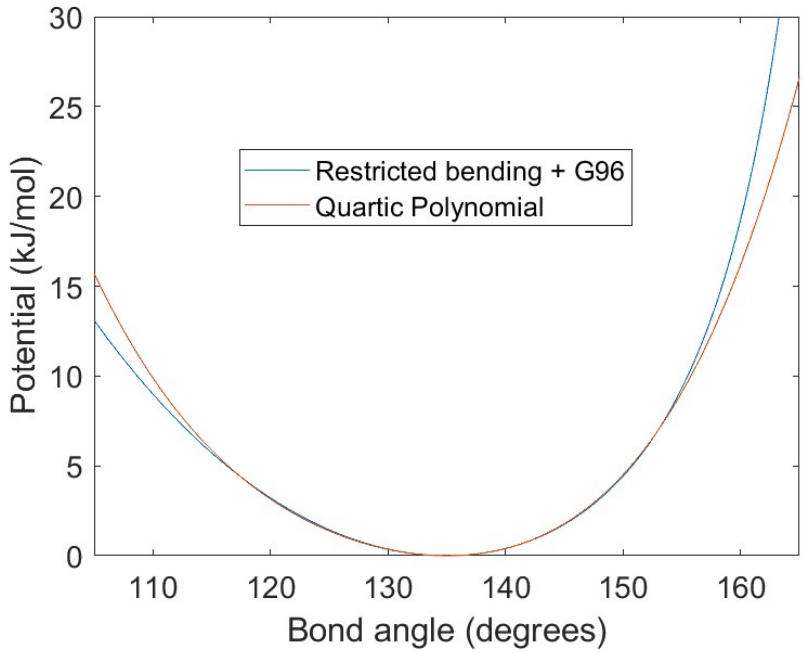

Figure S1: G96 + Restricted bending potential and the fit quartic polynomial potential

Figure S1 shows the G96 + Restricted bending potential and the quartic potential which is fit to it. It is apparent that the potentials are very similar for angles within three standard deviations of the mean (i.e. for 99.73% of the bond angles sampled in the simulation).

The resulting quartic potential is (where x is the deviation from the mean angle):

$f(x) = ax^4 + bx^3 + cx^2$

Coefficients (with 95% confidence bounds):

a = 103.6 (99.68, 107.5)

b = 37.84 (37.5, 38.19)

c = 48.78 (48.42, 49.14)

SI.07: Hydrophobic small molecules slow micelle formation:

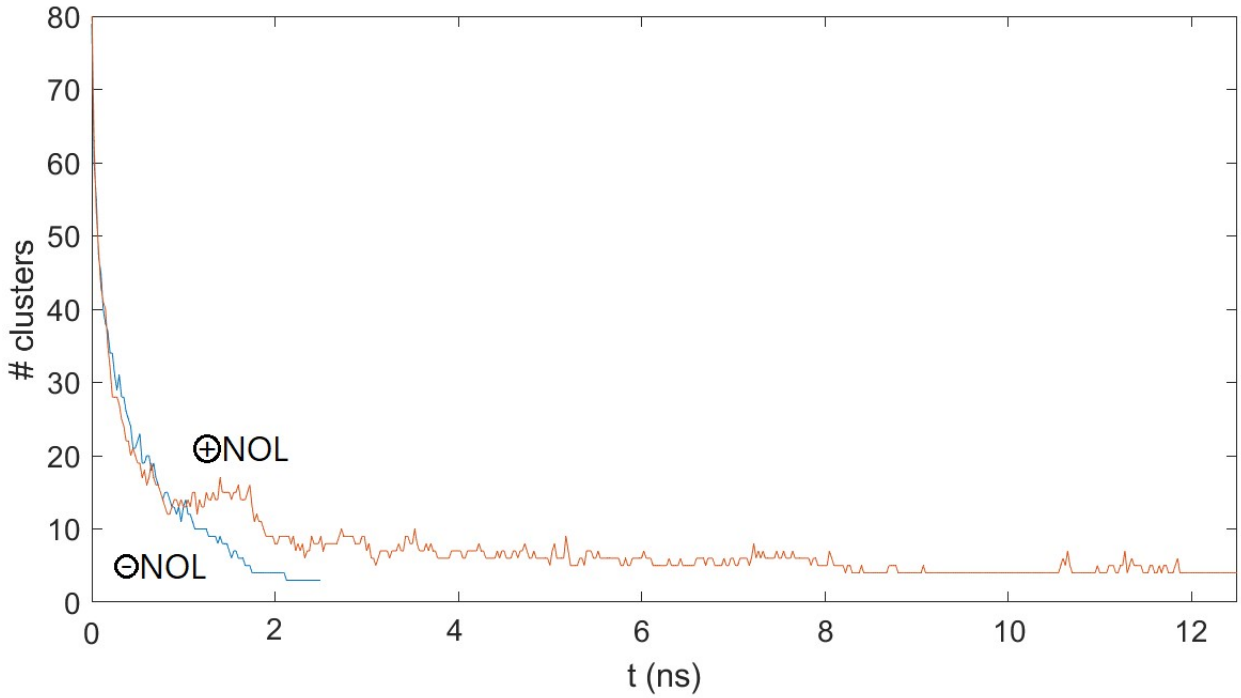

Figure S2: Formation of micelles in a system of 100 Span 20 surfactant molecules in the presence and absence of 5 mM NOL

SI.08: Variation of potential energies of interaction in sorbitan-ester surfactants:

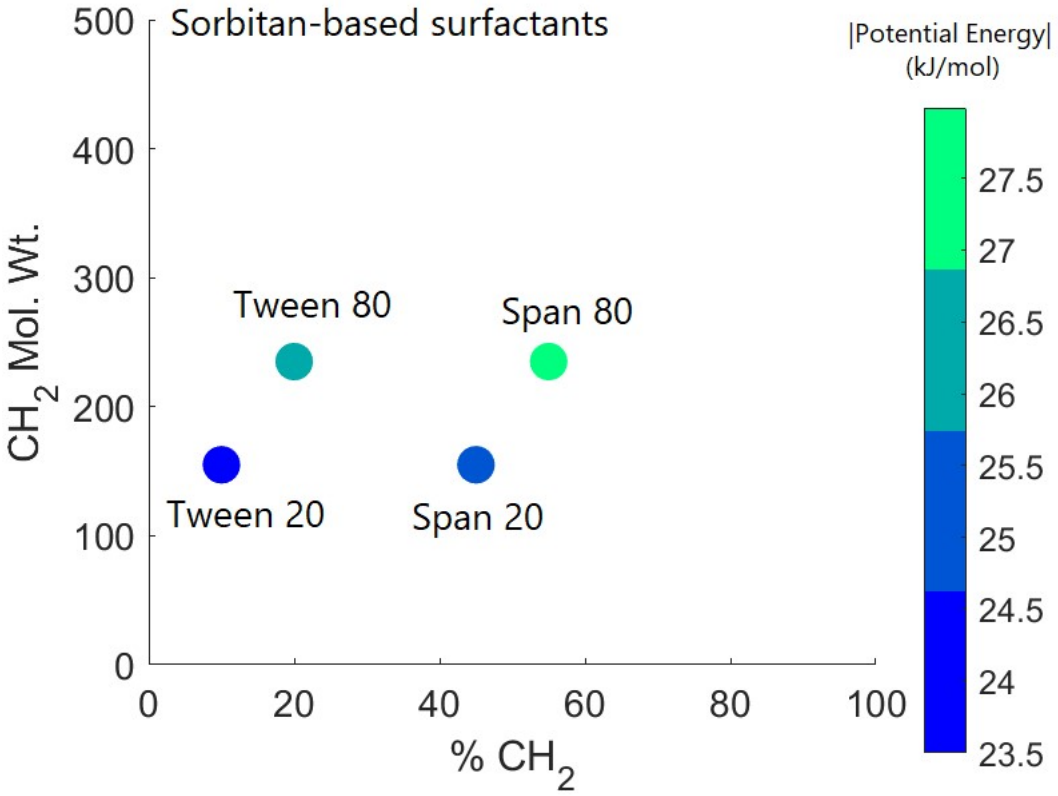

Figure S3: Potential energies of interaction between sorbitan-ester surfactants and NOL at equilibrium. As before, it can be seen that larger hydrophobic groups, and larger fraction of hydrophobic groups lead to stronger interactions

SI.09: Snapshots of the Span20-NOL system at equilibrium

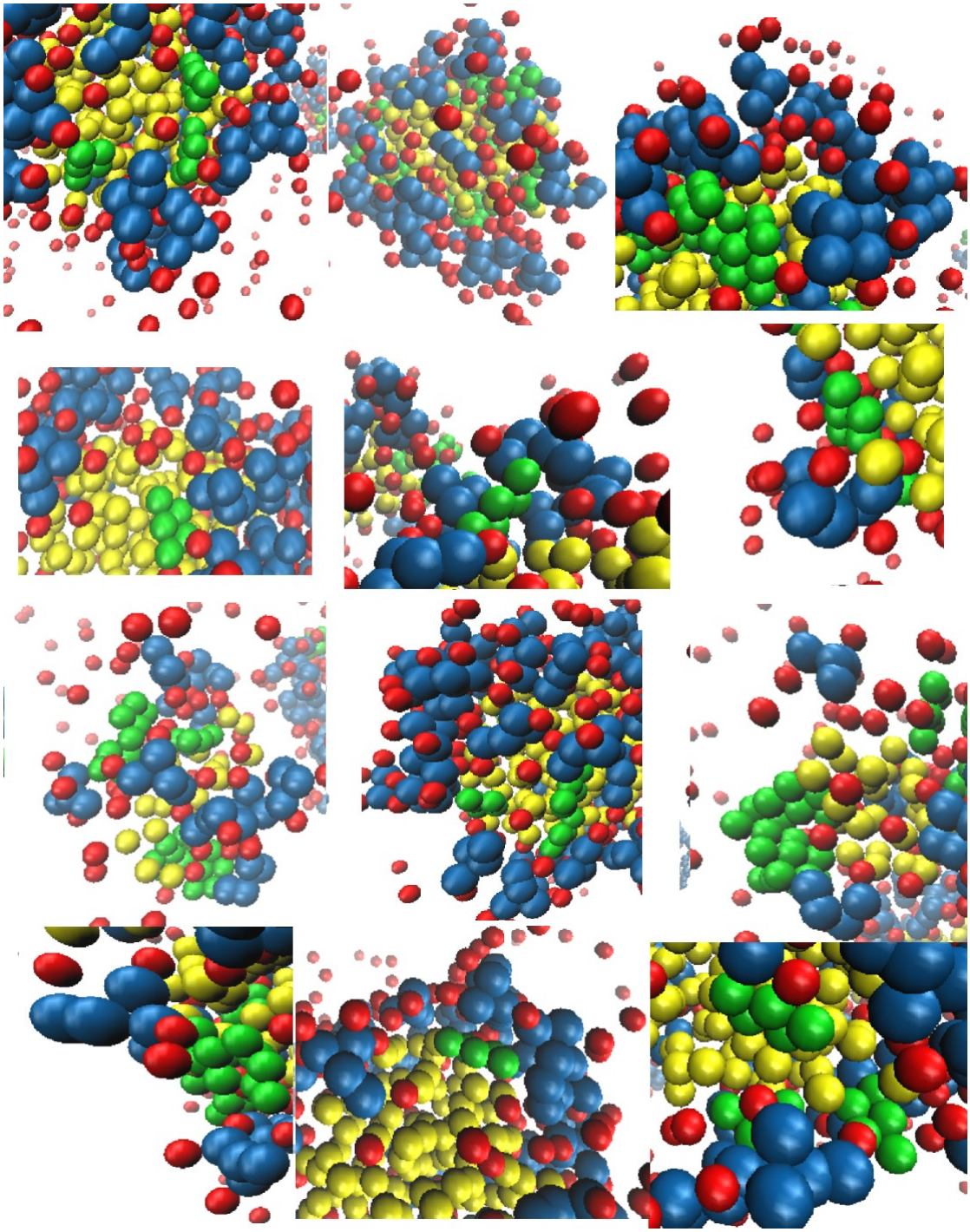

Figure S4: Snapshots of the Span 20 (2.5% v/v in water) and NOL (5 mM) system at equilibrium. NOL is shown in green, Span 20 hydrophilic beads are shown in blue, and Span 20 hydrophobic beads (alkyl) are shown in yellow. NOL is seen to occupy sites at the interface of the micelle core and corona. Water beads are not shown to aid viewing.

SI.10: Snapshots of the P85-NOL system at equilibrium

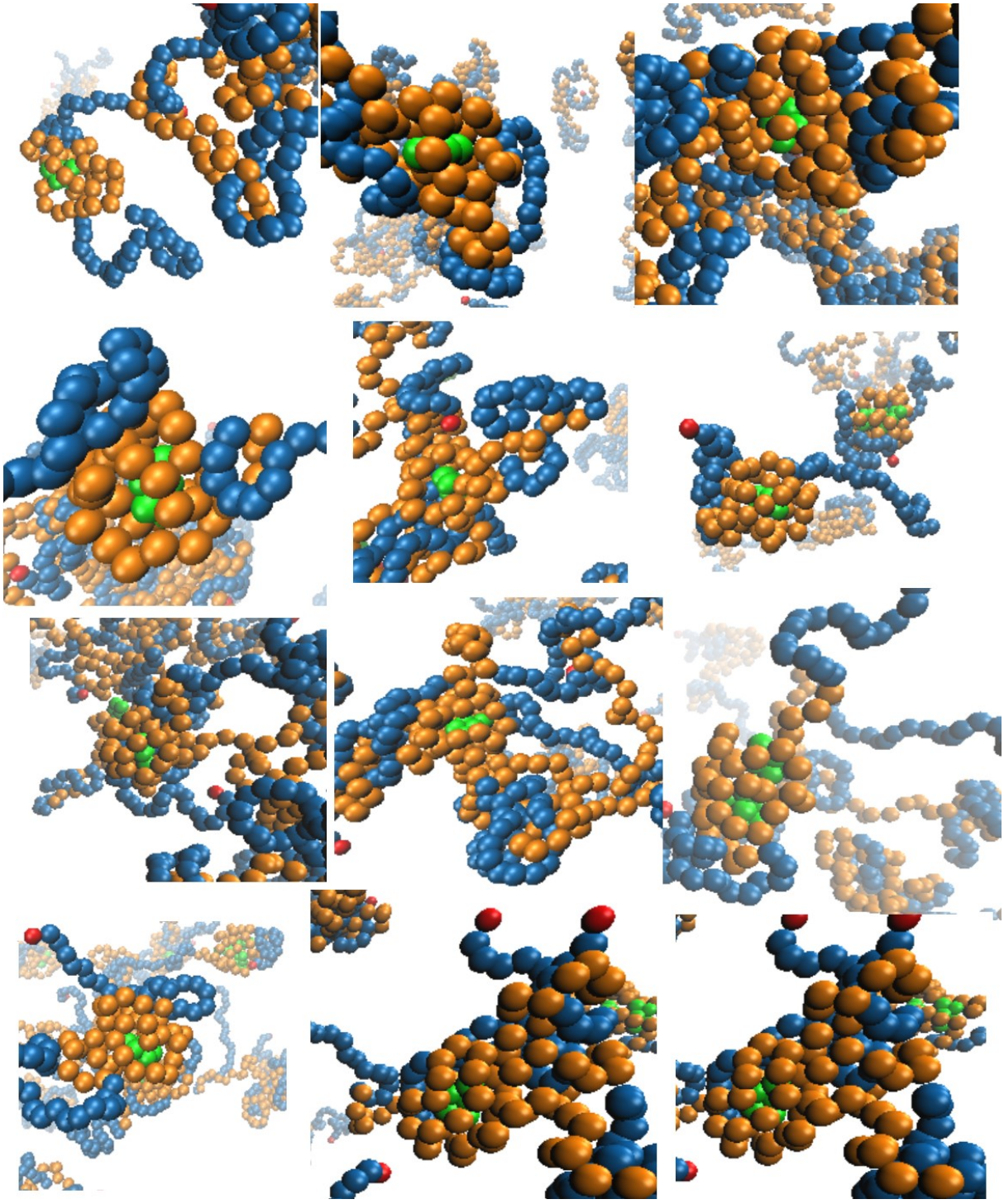

Figure S5: Snapshots of the P85 (2.5% v/v in water) and NOL (5 mM) system at equilibrium. NOL is shown in green, P85 hydrophilic beads (PEO) are shown in blue, and P85 hydrophobic beads (alkyl) are shown in orange. NOL is seen to occupy sites at the interface of the micelle core and corona. Water beads are not shown to aid viewing.

SI.11: Supplementary videos

Four supplementary videos are made available in electronic format as described below:

Video SV1: A video showing the increased agglomeration of surfactant B25 (2.5% v/v in water) micelles in the absence of constraints, when 5 mM NOL is added to the system

Video SV2: A video showing the increased agglomeration of surfactant P85 (2.5% v/v in water) micelles in the absence of constraints, when 5 mM NOL is added to the system

Video SV3: A video showing the lack of increased agglomeration of surfactant B25 (2.5% v/v in water) micelles in the presence of constraints, when 5 mM NOL is added to the system

Video SV4: A video showing the lack of increased agglomeration of surfactant P85 (2.5% v/v in water) micelles in the presence of constraints, when 5 mM NOL is added to the system

SI.12: Radial distribution function equilibration data

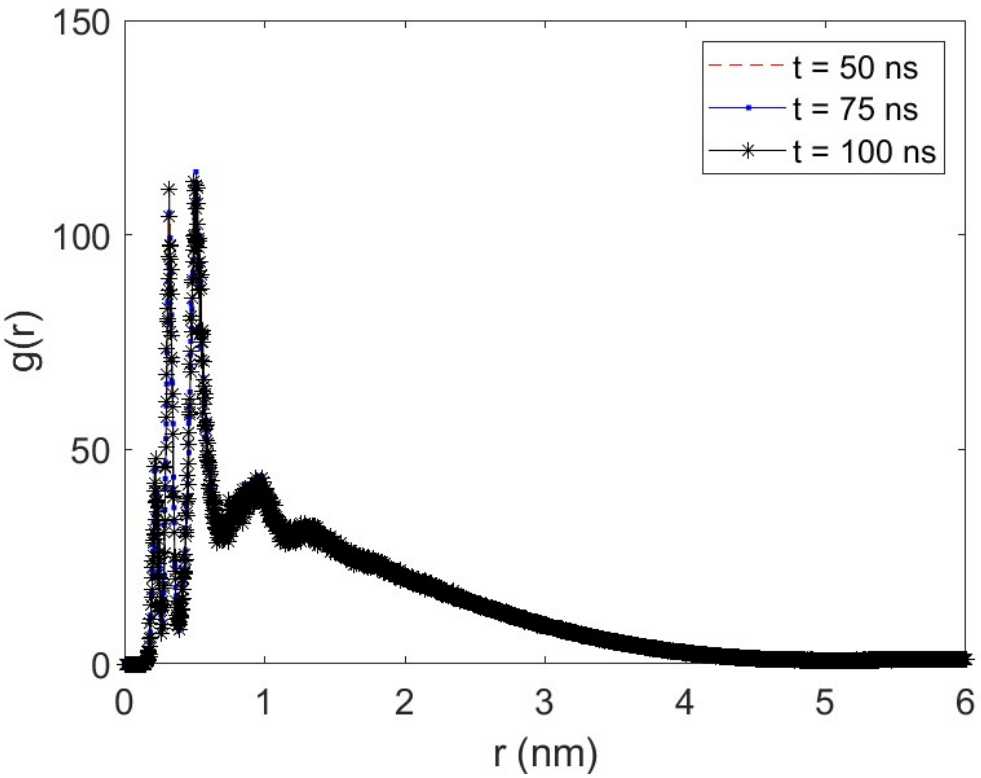

Figure S6: Span 20-Span 20 radial distribution functions showing equilibration. All data are averaged over 10 ns centered at the indicated time points.

SI.13 Box sizes and number of coarse-grained beads for various representative systems

Surfactant	# mol.	%EOL	# MAA	# W	# EOL	Total # beads	Total Volume (nm^3)	Box size (nm)
Alkyl-PEO Surfactants								
L10	100	0	715	33092	0	35137	4166	16
C10	100	0	779	36047	0	38256	4538	16
L23	100	0	1446	66922	0	70998	8425	20
C20	100	0	1281	59322	0	63133	7468	19
S20	100	0	1313	60800	0	64743	7654	10
B25	100	0	1710	79167	0	83707	9967	21
B25 (150)	150	0	2565	118750	0	125545	14945	25
PEO-PPO-PEO Surfactants (Pluronics)								
L31	100	0	1355	62753	0	66138	7898	20
L44	100	0	2621	121336	0	128287	15271	25
L61	100	0	2448	113314	0	119492	14261	24
L64	100	0	3551	164403	0	173884	20691	27
L92	100	0	4205	194697	0	205532	24503	29
P85	100	0	5350	247686	0	262266	31172	31
P85 (10% Ethanol)	100	0.1	5350	222918	24769	262267	31172	31
P85 (20% Ethanol)	100	0.2	5350	198149	49537	262266	31172	31
P85 (30% Ethanol)	100	0.3	5350	173380	74306	262266	31172	31
P85 (40% Ethanol)	100	0.4	5350	148612	99074	262266	31172	31
F68	100	0	9604	444653	0	472287	55961	38
F127	50	0	6966	322499	0	342395	40588	34
Sorbitan-ester Surfactants								
SPAN20 (100)	100	0	395	18285	0	19610	2301	13
SPAN20 (150)	150	0	592	27428	0	29400	3452	15
SPAN20 (200)	200	0	790	36571	0	39191	4603	17
SPAN20 (100, 10% Ethanol)	100	0.1	395	16457	1829	19611	2301	13
SPAN20 (100, 20% Ethanol)	100	0.2	395	14628	3657	19610	2301	13
SPAN20 (100, 30% Ethanol)	100	0.3	395	12800	5486	19611	2301	13
SPAN20 (100, 40% Ethanol)	100	0.4	395	10971	7314	19610	2301	13
SPAN80	100	0	489	22621	0	24340	2847	14
TWEEN20	100	0	1399	64787	0	69116	8154	20
TWEEN80	100	0	1493	69139	0	73862	8701	21

SI.14: Potential energies of interaction between surfactants and small molecules in free and immobilized systems

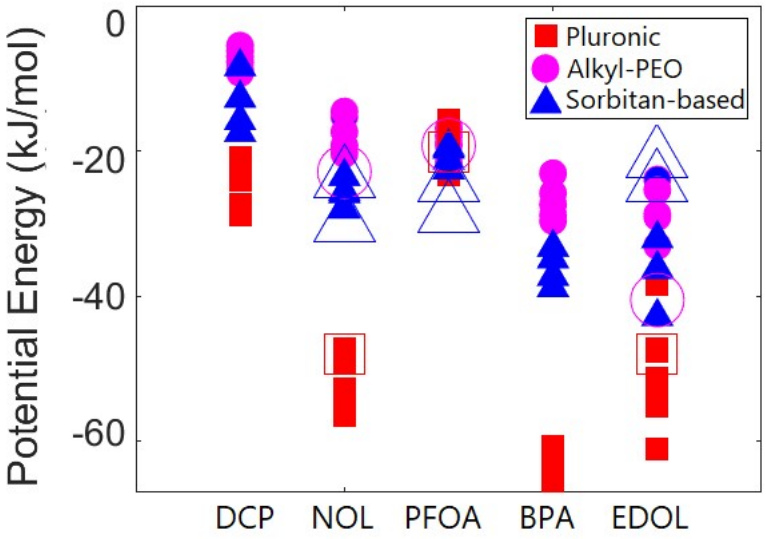

Figure S7: Potential energies of interaction between surfactant molecules in free (hollow markers) or immobilized micelles (solid markers) and small hydrophobic molecules. Each point represents one surfactant-hydrophobic molecule pair, with surfactants belonging to the same class having the same marker.

SI.14: References

[1] M. Almgren, P. Bahadur, M. Jansson, P. Li, W. Brown, and A. Bahadur, J. Colloid Interface Sci., 151, 157 (1992)

[2] S. A. Sanders and A. Z. Panagiotopoulos, J. Chem. Phys., 132(11), 114902 (2010)

[3] J. Nayem, Z. Zhang, A. Tomlinson, I. E. Zarraga, N. J. Wagner, Y. Liu, J. Pharm. Sci., 109(4), P1498-1508 (2020)